Development of Efficient 3D Models for Tilting Pad Journal Bearings

Roberto Conti, Amedeo Frilli, Emanuele Galardi,
Enrico Meli, Daniele Nocciolini, Luca Pugi, Andrea Rindi, and Stefano Rossin

Department of Industrial Engineering
University of Florence
via di S.Marta 3, 50139 Florence, Italy
roberto.conti@unifi.it,amedeo.frilli@stud.unifi.it,emanuele.galardi@unifi.it,enrico.meli@unifi.it,daniele.nocciolini@unifi.it,luca.pugi@unifi.it,andrea.rindi@unifi.it,stefano.rossin@ge.com
http://http://www.dief.unifi.it/

Abstract. This paper mainly focuses on the development of efficient three-dimensional (3D) models of TPJBs, able to in parallel simulate both the rotor dynamics behaviour and lubricant supply plant.
The proposed modelling approach tries to obtain a good compromease between the typical accuracy of standard 3D models and the high numerical efficiency of simpler and less accurate models.
In this work, the whole model has been developed and validated in collaboration with *Nuovo Pignone General Electric S.p.a.* which provided the required technical data. In particular, the experimental data are referred to a suitable lube oil console system, built at the GE testing center located in Massa-Carrara (MS, Italy) for the verification of such components.

1 Introduction

The authors aim to develop a model of Tilting Pad Journal Bearing including both the fluid dynamic and rotordynamic characteristics and preserving a competitive numerical efficiency. Therefore, the goal of this new model is to replace (partially or completely) both the classical lumped parameter models (poorly accurate for the modern industry requirements) and the complete 3D models (too time consuming).
The general layout of the model, consists of the following parts: TPJB model (including oil film model and pad dynamic model), rotor model, lubricant supply model (including duct model and sump model) and lube oil console model.
The pad model and the lubricant supply model are repeated n times depending on the considered Tilting Pad Journal Bearings, making the model highly modular. The whole model is built in the *COMSOL Multiphysics* ®4.2a and *MATLAB*®$R2011a$ environments.

2 General Architecture of the Model

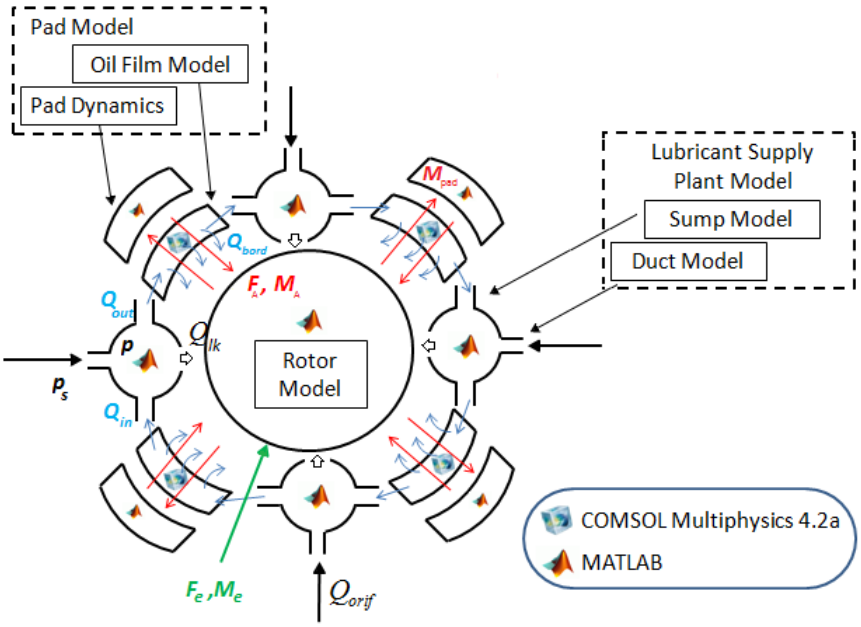

Fig. 1. General architecture scheme of the whole model.

An innovative feature of the developed architecture is the modularity of the approach, indeed, the behaviour of the pad/sump module can be repeated n times (where n represents the pads and sumps number), allowing the simulation of different bearings by adding or reducing the pad number.
To integrate different numerical solvers, the model solving architecture is divided into two parts: Partial Differential Equations (PDE) problem (the Reynolds equation for the oil film model is solved through the *COMSOL* solvers) and Ordinary Differential Equations (ODE) problem (in *MATLAB*, both the motion equations of rotor and pads and the 1D lumped equations of the lubricant supply model are solved).
This approach analyses separately the mechanical part and the fluid dynamics one reaching a good trade off between numerical efficiency and accuracy. Such decoupling is possible if the temporal integration step Δt is small enough; under this assumption, within the temporal interval Δt, the fluid dynamic problem is solved as steady-state (a simplified fluid dynamic model is used, neglecting turbolent state flow). This hypothesis is acceptable if the oil film thickness is thin enough (compared to the other directions [2]).
An implicit, variable order and variable step ODE-solver, suitable for stiff problems (conventionally defined as *ode15s*), is used to simulate the time-dependent

part [5], [6].
The CFD oil film model (steady) reaches the solution using an iterative non linear solver type based on Newtonian methods [7]. The linear problem arising from the non linear solver are solved through an iterative method (*BicGStab* [8]).
As regards the mesh, it has been realized by means of bidimensional elements (this assumption is verified by the hypothesis underlying the Reynolds equation), to maintain acceptable performances and accurate results [20].

3 Model Description

In the following sections the different parts of the model will be described in detail.

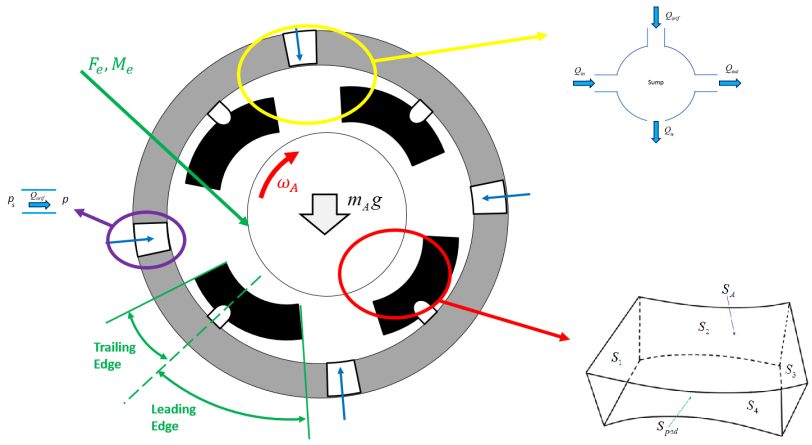

Fig. 2. Components of the whole model.

In Figure 1 and 2, the S_A, S_{pad} represent respectively the rotor and pad surfaces, while S_1, S_3 are the inlet and outlet oil sections of the control volume; finally S_2, S_4 are the lateral leakage surfaces of the control volume.

3.1 TPJB Model

In this research paper, basing on the technical data provided by *Nuovo Pignone General Electric S.p.a.*, the CFD analysis is performed on the Journal Bearing JB200 (where the rotor diameter is 200 mm, the external diameter is 395 mm and the thickness is 170 mm) with 4 tilting pads set in the "X" configuration.
According to the model architecture, the pad model is divided into: oil film model and pad dynamic model.

The Oil Film Model The model inputs are defined by the rotor and pad kinematical quantities $\underline{x}_A = (x_A\ y_A\ z_A\ \alpha_A\ \beta_A\ \gamma_A)^T$, $\underline{\dot{x}}_A = (\dot{x}_A\ \dot{y}_A\ \dot{z}_A\ \dot{\alpha}_A\ \dot{\beta}_A\ \dot{\gamma}_A)^T$, $\underline{x}^i_{pad} = (\gamma^i_{pad})$ and $\underline{\dot{x}}^i_{pad} = (\dot{\gamma}^i_{pad})$.
The model is supposed time-independent and thus a steady-state problem is solved.
The oil film thickness h is given by:

$$\underline{h} = h\left(x_A, y_A, z_A, \alpha_A, \beta_A, \gamma_A, \gamma_{pad}, R_p, R_{rot}\varphi, \chi\right) \tag{1}$$

where φ, χ are the angles describing the oil film thickness orientation in a spherical reference system, R_p is the internal pad radius and R_{rot} is the rotor radius.
The forces that the oil film acts on rotor and pads can be calculated as follows:

$$\underline{F}_A = \int_{S_A} \sigma\ \underline{n}_A dS_A, \qquad \underline{F}^i_{pad} = \int_{S_{pad}} \sigma\ \underline{n}_{pad} dS_{pad}. \tag{2}$$

where σ is the fluid stress tensor and $\underline{n}_A$, $\underline{n}_{pad}$ are the outgoing unitary vectors respectively from the rotor surface S_A and the pad surface S_{pad}.
The momenta acting on the rotor and pads can be calculated according to the following equations:

$$\underline{M}_A = \int_{S_A} \underline{r}_A \times \sigma\ \underline{n}_A dS_A, \qquad \underline{M}^i_{pad} = \int_{S_{pad}} \underline{r}_{pad} \times \sigma\ \underline{n}_{pad} dS_{pad}. \tag{3}$$

The oil flow rates Q^i_{in}, Q^i_{out}, $Q^i_{bord,l}$ and $Q^i_{bord,r}$ are described as follows:

$$\begin{array}{ll} Q^i_{in} = \int_{S_3} \rho \underline{v}\ \underline{n}_3 dS_3, & Q^i_{out} = \int_{S_1} \rho \underline{v}\ \underline{n}_1 dS_1, \\ Q^i_{bord,l} = \int_{S_2} \rho \underline{v}\ \underline{n}_2 dS_2, & Q^i_{bord,r} = \int_{S_4} \rho \underline{v}\ \underline{n}_4 dS_4, \end{array} \tag{4}$$

where $\underline{v}$ represents the oil film velocity and $\underline{n}_1$, $\underline{n}_2$, $\underline{n}_3$, $\underline{n}_4$ are the outgoing unitary vectors respectively from surfaces S_1, S_2, S_3 and S_4 (see Figure 2).
The model outputs are the forces $F_{x,A}$, $F_{y,A}$, $F_{z,A}$ and momenta $M_{x,A}$, $M_{y,A}$, $M_{z,A}$ acting on the rotor (subscript A) and on the pad $M^i_{z,pad}$ (subscript pad) and the inlet/outlet flow rates Q^i_{in}, Q^i_{out} from the pad edges and the flow rate $Q^i_{bord,l}$ and $Q^i_{bord,l}$ exiting from the pad side edges.

Pad Dynamics Model The Pad Dynamics Model describes the dynamics of rotation around the cylindrical pad pivot (then presents a single DOF). The inputs are represented by the momentum $M^i_{z,pad}$ acting on the pad. The geometry of the pad is shown in Figure 2.
The pad motion equation is given by:

$$I^i_{pad}\ddot{\gamma}^i_{pad} = M^i_{z,pad}; \tag{5}$$

where γ indicates the rotation around the pad axis z, I^i_{pad} defines the pad polar moment of inertia, and $M^i_{z,pad}$ is calculated by equation 3.
The outputs are the pad position γ^i_{pad} and speed $\dot{\gamma}^i_{pad}$.

3.2 The Rotor Model

The proposed model is based on a centrifugal compressor (called 3BCL1005) used to liquefy natural gas, directly coupled to a condensing-type steam turbine driver, where the characteristics are provided by *Nuovo Pignone General Electric S.p.a.* and is tested in a GE testing center located in Massa-Carrara (MS, Italy).
The inputs are defined by the forces $F_{x,A}$, $F_{y,A}$, $F_{z,A}$ and momenta $M_{x,A}$, $M_{y,A}$, $M_{z,A}$ acting on the rotor and possible external loads and torques (F_e, M_e).
The dynamics of the rotor considers the following 6 DOFs: rotation around the symmetry axis (z-axis), translation along the symmetry axis (z-axis) and traslations and rotations around the other two axes (x-axis and y-axis) approximating the rotor model to a rigid disk gyroscopic model (since the polar moment of inertia I_p is greater than the transversal moment of inertia I_t).
Hence, the motion equations (6), (7), (8) can be written:

$$I_p \ddot{\gamma}_A = \sum_{i=1}^{n} M_{z,A}^i + C_{mot} + M_{z,e}, \tag{6}$$

$$m_A \ddot{z}_A = \sum_{i=1}^{n} F_{z,A}^i + F_{z,e}, \tag{7}$$

$$M_k \begin{Bmatrix} \ddot{x}_A \\ \ddot{\beta}_A \\ \ddot{y}_A \\ \ddot{\alpha}_A \end{Bmatrix} + \dot{\gamma_A} G_k \begin{Bmatrix} \dot{x}_A \\ \dot{\beta}_A \\ \dot{y}_A \\ \dot{\alpha}_A \end{Bmatrix} = \begin{Bmatrix} \sum_{i=1}^{n} F_{x,A}^i + F_{x,e} \\ \sum_{i=1}^{n} M_{y,A}^i + M_{y,e} \\ \sum_{i=1}^{n} F_{y,A}^i - m_A g + F_{y,e} \\ \sum_{i=1}^{n} M_{x,A}^i + M_{x,e} \end{Bmatrix}, \tag{8}$$

where, n defines the pad number, m_A the rotor mass, C_{mot} is the motor torque, g is the modulus of the gravity acceleration vector, M_k and G_k represent respectively the mass and gyroscopic effect matrices.
Finally, $F_{x,A}^i$, $F_{y,A}^i$, $F_{z,A}^i$, $M_{x,A}^i$, $M_{y,A}^i$, $M_{z,A}^i$ are the forces and momenta acting on the rotor and $F_{x,e}$, $F_{y,e}$, $F_{z,e}$, $M_{x,e}$, $M_{y,e}$, $M_{z,e}$ are the possible external forces and momenta.
The outputs of the model are the rotor position x_A, y_A, z_A, α_A, β_A, γ_A, and velocities $\dot{x}_A$, $\dot{y}_A$, $\dot{z}_A$, $\dot{\alpha}_A$, $\dot{\beta}_A$, $\dot{\gamma}_A$.

3.3 Lubricant Supply Model

The lubricant supply model has been realized following the Bond-Graph approach for the modelling of general multiphysics system [18], [19]. The lubricant supply model represents the supply and leakage of the system and it is divided in two components: the Duct model and the Sump model.

Duct Model The Duct Model describes the supply and leakage flow rates inside the sump.
The inputs are the sump pressure p^i, the supply pressure p_s and the environment

pressure p_{env}.
This model is based on the Bond-Graph theory of lumped parameters modelling [18], [19], which implements elements of T (*through*) type (resistive elements). It represents the leakages and supply.
The duct expressions are thence shown; Q^i_{orif} and Q^i_{lk} are defined according to the following laws:

$$Q^i_{orif} = A_0 C_d \sqrt{\frac{2}{\rho}(p_s - p^i)}, \qquad Q^i_{lk} = A_{lk} C_{dlk} \sqrt{\frac{2}{\rho}(p^i - p_{env})}, \tag{9}$$

where A_0 is the duct section, C_d is the duct flow coefficient, A_{lk} is the sump section, C_{dlk} is the sump flow coefficient, ρ is the lubricant density and p_{env} is the environment pressure.
The outputs are the supply and leakage flow rates, respectively Q^i_{orif}, Q^i_{lk}.

Sump Model The Sump Model describes the balance of the flow rates inside the sump. The inputs are defined by the the inlet/outlet flow rates Q^i_{in}, Q^i_{out} from the pad edges, the supply and leakage flow rates, respectively Q^i_{orif}, Q^i_{lk}. The sump scheme is shown in Figure 2; in particular, a sump is interposed between two adjacent pads. This model is based on the Bond-Graph theory of lumped parameters modelling [18], [19], which implements elements of A (*across*) type (capacitive elements). The constitutive equation of this element is:

$$\frac{dp^i}{dt} = \frac{K}{Vol}\left(Q^i_{in} - Q^i_{lk} - Q^i_{out} + Q^i_{orif}\right), \tag{10}$$

in which K is the Bulk module, Vol is the sump volume obtained by geometric measurements. This equation can be used considering that in this area (inside the bearing) the pressure is approximatively constant in the whole volume because the effects pruduced by the rotor on the sump are neglected. Q^i_{in} is the input flow rate from the previous pad, Q^i_{lk} represents the flow rate losses, Q^i_{out} is the output flow rate from the sump to the next pad, Q^i_{orif} is the flow rate introduced from outside.
The output of the model is the sump pressure p^i.

4 Experimental Data Description

The Tilting Pad Journal Bearing model has been carried out and validated by the technical data of the $JB200$ (provided by Kingsbury), having 4 tilting pads with a "X" configuration. The TPJBs are installed on a 3BCL1005 centrifugal compressor provided by *Nuovo Pignone General Electric S.p.a.*. The main features and operating conditions of the TPJB and of the rotor are shown in Table 1.

The TPJB model has been validated through a comparison with experimental data provided by General Electric Oil & Gas and coming from experimental testing of the entire system described in Figure 3 carried out at the GE testing center located in Massa-Carrara (MS, Italy).

Pad model:	
Journal radius	100 [mm]
Pad thickness	35 [mm]
Bearing lenght	170 [mm]
Bearing radial clearance	0.254 [mm]
Pad radial clearance	0.371 [mm]
Rotor model:	
Young's modulus E	210 [GPa]
Poisson's ratio	0.31
Rotor mass m_A	5530 [kg]
Rotational shaft speed $\dot{\gamma}_A$	$3777 \div 3813$ [rpm]
Static load $m_A g$	54249.3 [N]
Polar moment of inertia I_p	$4[kg \cdot m^2]$
Transversal moment of inertia I_t	$420[kg \cdot m^2]$
envient pressure p_{env}	1 [bar]

Table 1. Bearing geometry and operating conditions.

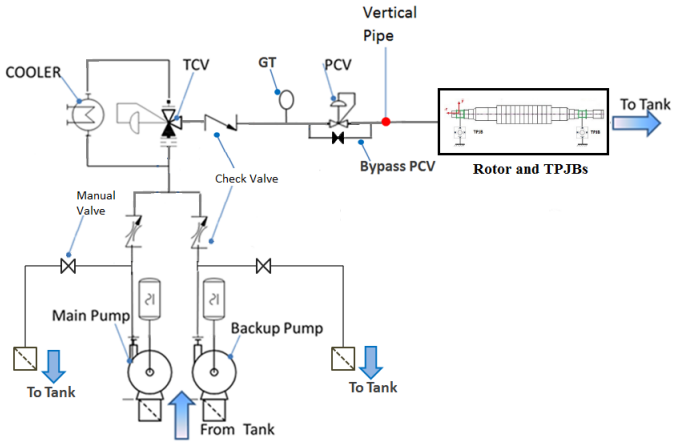

Fig. 3. Simple scheme of the lubrication testing system in Massa-Carrara.

The experimental data are obtained evaluating the measured drop pressure $p_s^{meas} - p_{env}$ and flow rate Q_{orif}^{meas} (single value associated to the whole bearing considered) at a steady state condition defined by temperature T^{meas} and rotational velocity of the rotor $\dot{\gamma}_A^{meas}$. In addition, two levels of temperatures are considered: $50°C$, which is the nominal operating temperature, and $65°C$, considered high temperature.
The results are referred to a single Tilting Pad Journal Bearing (the one nearest to the rotor center of mass) exclusively for reasons of synthesis; the measures, however, were made on both the TPJBs and the test results concern the whole system.

The measured flow rate Q_{orif}^{meas} concerns the whole tilting pad journal bearing and consequently is validated by the sum of the flow rates adduced on the n sumps:

$$Q_{orif} = \sum_{i=1}^{n} Q_{orif}^{i} \tag{11}$$

Q_{orif} is the variable to be considered in the model and will be compared to Q_{orif}^{meas}. The ideal test case are obtained applying both the ideal monodimensional formula [17] and the GE NP formula:

$$\begin{aligned} Q_{orif}^{id} &= A_0 C_d \sqrt{\tfrac{2}{\rho}\left(p_s^{meas} - p_{env}\right)}, \\ Q_{orif}^{GENP} &= D^2 k_{GENP} \tfrac{\beta^2}{\sqrt{1-\beta^2}} \cdot \sqrt{\tfrac{(p_s^{meas} - p_{env})}{\rho}}, \end{aligned} \tag{12}$$

where Q_{orif}^{id} and Q_{orif}^{GENP} are the computed flow rates considering the whole bearing as an ideal orifice, $p_s^{meas} - p_{env}$ is the measured drop pressure, C_d is the flow coefficient, A_0 is the orifice area, D is the pipe diameter, β is the ratio between the orifice and pipe diameters and k_{GENP} is a numeric adimensional constant. The first equation of the 12 is usually used to model the Tilting Pad Journal Bearings behaviour from the hydraulic point of view; while the second equation is currently used within *Nuovo Pignone General Electric S.p.a.* for hydraulic modelling of the TPJBs. The values of the above mentioned parameters are provided by *Nuovo Pignone General Electric S.p.a.*.

5 Validation and Results

In this section, the authors present the comparison between the drop pressure $p_s^{meas} - p_{env}$ curve and the flow rate Q_{orif} curve (simulated and experimental). In Figure 4 the flow rate results obtained with the proposed model are shown, compared to the previous experimental data and the ideal and GE NP formulas. The flow rates Q_{orif}^{meas}, Q_{orif}^{GENP} and Q_{orif}^{id} concern the whole Tilting Pad Journal Bearing and consequently are validated respect to the sum of the flow rates ($Q_{orif} = \sum_{i=1}^{n} Q_{orif}^{i}$) adduced on the n sump.

$Q_{orif}^{'}$ is obtained by the interpolation of the points Q_{orif}, which are numerically derived from the whole model (achieving good results in terms of accuracy). The $Q_{orif}^{'}$ fits better to the measured data, compared to the ideal and GE NP curves. The maximum relative errors shown in Figure 4 are highlighted in Table 2 (it is worth to note that the maximum relative errors can be found at high $p_s^{meas} - p_{env}$ and Q_{orif}).

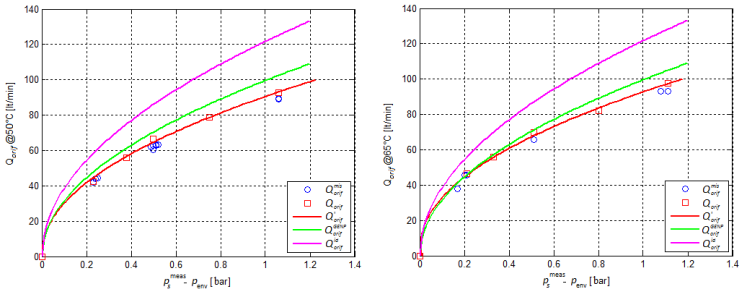

Fig. 4. Proposed model results compared to experimental data for different formulae comparisons.

	proposed model	GE NP model	ideal model
$50°C$	3.36%	13.43%	38.59%
$65°C$	3.77%	10.41%	29.91%

Table 2. Maximum relative errors.

6 Conclusions and Future Developments

An innovative TPJB modelling approach is described in this paper to increase the result accuracy with reduced computational time. The coupling between the fluid dynamics and rotordynamics effects is realized with the interaction between a 3D modelling and model parts still treated with 1D equations (the 1D formulation is implemented in the submodel that less affect the model accuracy).
The proposed model aims to obtain a compromise between the accuracy of complete 3D models and the efficiency of lumped parameters models.
The whole model has been developed and validated in collaboration with *Nuovo Pignone General Electric S.p.a.* which provided the required technical data and the test results. The results show a good agreement with experimental data (good accuracy), while the computation time are reduced compared to a totally 3D model (good efficiency). The following future developments stem from this research activity:

- analysis of the heat exchange inside the oil film and other components;
- implementation of flexibility in the rotor and pads models;
- implementation of the proposed model in rotor trains and more complex supply plants.

Acknowledgments

Authors wish to thank all the people of *Nuovo Pignone General Electric S.p.a.* that have cooperated to this project for their helpful contribution and competence.

References

1. G. Genta, *Vibration of Structures and Machines - Practical Aspects*, Second Edition, Springer-Verlag.
2. B. J. Hamrock, *Fundamentals of Fluid Film Lubrication*, Mc-Graw-Hill-International Editions.
3. T. Almqvist, S. B. Glavatskih, R. Larsson, *THD Analysis of Tilting Pad Thrust Bearing Comparison Between Theory and Experiments*, Journal of Tribology, Vol. 122, 2000.
4. H. Tripp, B. Murphy, *Eccentricity Measurements on a Tilting-Pad Bearing*, Volume 28,2, 217-224, ASLE transactions.
5. P. Bogacki, L. F. Shampine, *A 3(2) pair of Runge-Kutta formulas*, Appl. Math. Letters, Vol. 2, 1989, pp. 321-325.
6. J. R. Dormand, P. J. Prince, *A family of embedded Runge-Kutta formulae*, J. Comp. Appl. Math., Vol. 6, 1980, pp. 19-26.
7. C. T. Kelley, *Solving Nonlinear Equations with Newton's Method*, no 1 in Fundamentals of Algorithms, SIAM, 2003. ISBN 0-89871-546-6.
8. H. A. V. d. Vorst, *Bi-CGSTAB: A Fast and Smoothly Converging Variant of Bi-CG for the Solution of Nonsymmetric Linear Systems*, SIAM J. Sci. and Stat. Comput. 13 (2): 631-644, 1992.
9. J. Bouyer, M. Fillon, *On the Significance of Thermal and Deformation Effects on a Plain Journal Bearing Subjected to Severe Operating Conditions*, ASME J. Tribol., Vol. 126, No. 4, pp. 819-822, ISSN: 0742-4787, 2004.
10. Q. Chang, P. Yang, Y. Meng, S. Wen, *Thermoelastohydrodynamic analysis of the static performance of tilting-pad journal bearings with the Newton-Raphson method*, Tribol. Int., Vol. 35, No. 4, pp. 225-234, ISSN: 0301-679X, 2002.
11. D. Brugier, M.T. Pasal, *Influence of elastic deformations of turbo-generator tilting pad bearings on the static behavior and on the dynamic coefficients in different designs*, ASME J. Tribol., Vol. 111, No. 2 , pp. 364-371, ISSN: 0742-4787, 1989.
12. F. P. Incropera, D. P. DeWitt, *Fundamentals of Heat and Mass Transfer*, Fourth Edition, John Wiley & Sons, 1996.
13. S. Piffeteau, D. Souchet, D. Bonneau, *Influence of Thermal and Elastic Deformations on Connecting-Rod End Bearing Lubrication Under Dynamic Loading*, ASME J. Tribol., Vol. 122, No. 1, pp. 181-191, ISSN: 0742-4787, 2000.
14. A. Kumar, J.F. Booker, *A finite element cavitation algorithm: Application/validation*, ASME J. Tribol., Vol. 107, pp. 253-260, ISSN: 0742-4787, 1991.
15. D. Bonneau, M. Hajjam, *Modélisation de la rupture et de la formation des films lubrifiants dans les contacts élastohydrodynamiques*, Revue Européenne des Eléments Finis, Vol. 10, No. 6-7, pp. 679-704, ISSN: 1250-6559, 2001.
16. Y. L. Wang, Z. S. Liu, W. J. Kang, J. J. Yan, *Approximate analytical model for fluid film force of finite length plain journal bearing*, Proc. IMechE Vol. 226 Part C: J. Mechanical Engineering Science, 2011.
17. F. Kreith, *The CRC Handbook of Mechanical Engineering*, ISBN0-8493-9418-X, 1997.
18. L. Yu, X. Qi, *Bond-Graph Modelling in System Engineering*, International Conference on Systems and Informatics, 2012.
19. A. Malik, A. Khurshid, *Bond Graph Modelling and Simulation of Mechatronic Systems*, Proceedings IEEE INMIC, 2003.
20. G. Strang, G. Fix, *An Analysis of the Finite Element Method*, Englewood Cliffs, Prentice-Hall, 1973.